Alkyl–π Functional Molecular Gels: Control of Elastic Modulus and Improvement of Electret Performance

Akito Tateyama,[a,b] Kazuhiko Nagura,[b] Masamichi Yamanaka,[c] and Takashi Nakanishi*[a,b]

[a] Mr. A. Tateyama, Prof. Dr. T. Nakanishi
Division of Soft Matter, Graduate School of Life Science
Hokkaido University
Kita 10, Nishi 8, Kita-ku, Sapporo 060-0810, Japan
E-mail: NAKANISHI.Takashi@nims.go.jp
[b] Mr. A. Tateyama, Dr. K. Nagura, Prof. Dr. T. Nakanishi
Research Center for Materials Nanoarchitectonics (MANA)
National Institute for Materials Science (NIMS)
1-1 Namiki, Tsukuba 305-0044, Japan
[c] Prof. Dr. M. Yamanaka
Meiji Pharmaceutical University (MPU)
2-522-1 Noshio, Kiyose 204-8588, Japan

Abstract:

The development of optoelectronically-active soft materials is drawing attention to the application of soft electronics. A room-temperature solvent-free liquid obtained by modifying a π-conjugated moiety with flexible yet bulky alkyl chains is a promising functional soft material. Tuning the elastic modulus (*G′*) is essential for employing optoelectronically-active alkyl–π liquids in deformable devices. However, the range of *G′* achieved through the molecular design of alkyl–π liquids is limited. We report herein a method for controlling *G′* of alkyl–π liquids by gelation. Adding 1 wt% low-molecular-weight gelator formed the alkyl–π functional molecular gel (FMG) and increased *G′* of alkyl–π liquids by up to seven orders of magnitude while retaining the optical properties. Because alkyl–π FMGs have functional π-moieties in the gel medium, this new class of gels has a much higher content of π-moieties of up to 59 wt% compared to conventional π-gels of only a few wt%. More importantly, the gel state has a 23% higher charge-retention capacity than the liquid, providing better performance in deformable mechanoelectric generator-electret devices. The strategy used in this study is a novel approach for developing next-generation optoelectronically-active FMG materials.

There is increasing demand for devices with flexible characteristics such as stretchability, foldability, and deformability for healthcare applications, wearable sensing, and soft robotics.[1–7] Sophisticated optoelectronically-active soft materials with appropriate viscoelasticity are necessary for developing such devices.[8,9] Alkyl–π functional molecular liquids (FMLs), which are designed as bulky yet flexible branched-alkyl chains attached to a π-conjugated moiety, are a promising optoelectronically-active soft material.[10–13] In addition to their liquid fluidity, alkyl–π FMLs can maintain the optoelectronic functions inherent in the π-conjugated moieties even in the bulk neat liquid state.

Attempts have been made to apply alkyl–π FMLs to practical devices such as microfluidic light-emitting diodes[14,15] and stretchable mechanoelectric generator-electret devices (MEGs).[16–19] Liquid fluidity has the advantage of shape adaptability; however, there are concerns about liquid leakage and bleeding from a support membrane with adsorbed liquid. Furthermore, improvements such as increased charge retention capability and elimination of the need for support materials to immobilize liquid electrets are required, especially for MEG applications. One possible solution to meet these demands is to tune the elastic modulus (G') while preserving the softness and optoelectronic functionality of the alkyl–π FMLs. So far, the complex viscosity ($|\eta^*|$) and G' of alkyl–π FMLs have been controlled by altering the substitution position and the length of the branched-alkyl chains.[20,21] The strategy of increasing G' has also been demonstrated in the case of alkyl–π conjugated polymer fluids,[22–24] where G' can be controlled by more than five orders of magnitude depending on the branched alkyl chain length.[23] However, since arranging the chemical structure for every alkyl–π conjugated polymer fluid is a complicated and time-consuming process, a simple method of controlling G' over a broader range is required to expand the usefulness of alkyl–π FMLs.

In the present study, we developed alkyl–π functional molecular gels (FMGs), because gelation is the most helpful technique for dramatically adjusting G' of liquids.[25–28] Since gelation has been a blind spot in the research field of alkyl–π FMLs,[10–13] we first focused on investigating the fundamental properties of the formed gels that use a low-molecular-weight gelator. As for device applications, we focused on MEGs. Alkyl–π FMLs have an electroactive π-moiety wrapped with insulating alkyl chains, making them suitable for storing electrostatic charges inside the liquid and

functioning as liquid electrets.[16–18] This study revealed that gelation improves electret performance and eliminates the need for supporting materials in MEG devices.

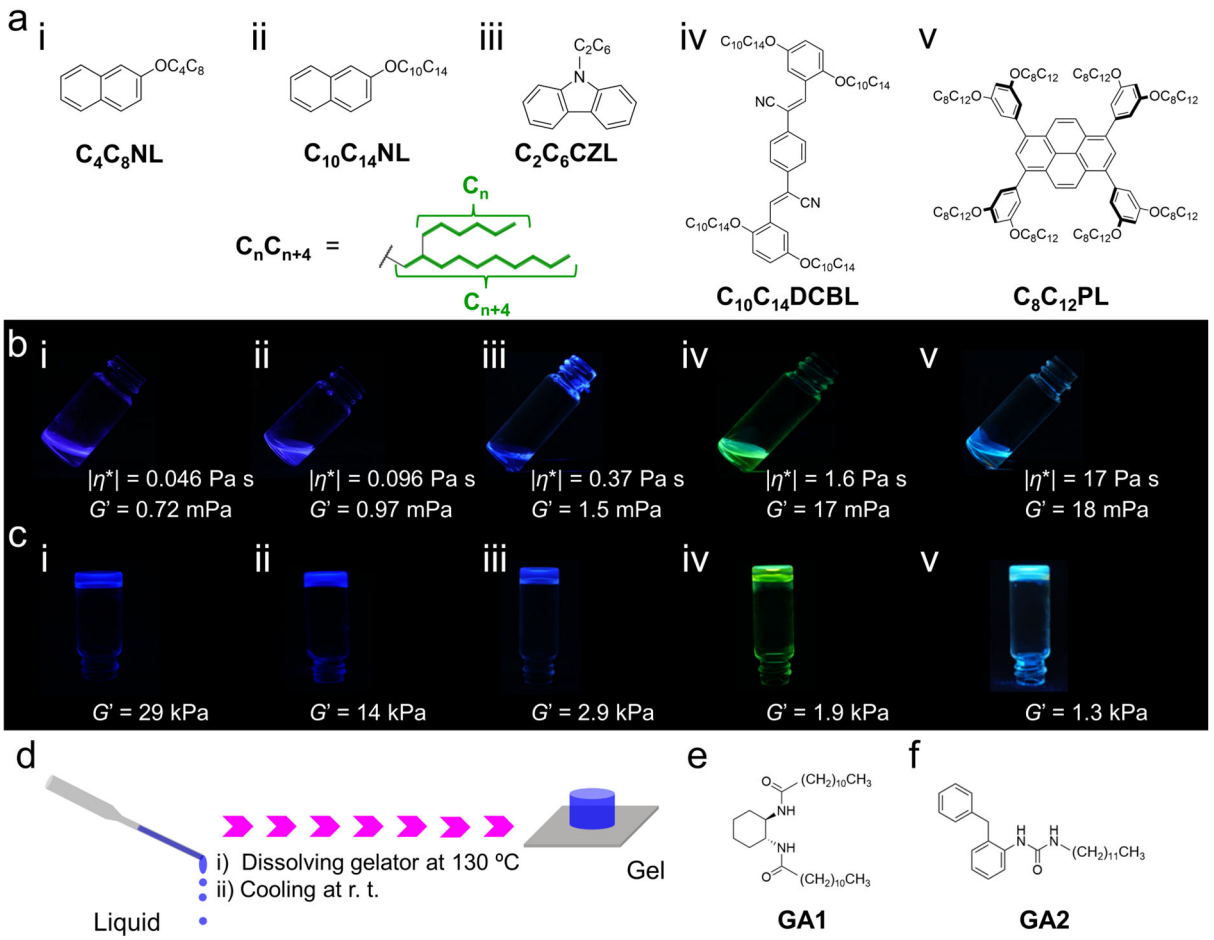

Figure 1. a) Chemical structure of alkyl–π FML compounds utilized in this study, i) **C₄C₈NL**, ii) **C₁₀C₁₄NL**, iii) **C₂C₆CZL**, iv) **C₁₀C₁₄DCBL**, and v) **C₈C₁₂PL**. Photo images of b) neat liquid state of the alkyl–π FML compounds (i–v), and c) their gels formed with 1 wt% **GA1**, taken under 365 nm UV light irradiation. Their complex viscosity ($|\eta^*|$) and elastic modulus (G') measured at 25 °C and angular frequency of ω = 0.1 rad s^{-1} are shown in b) and c). d) Scheme of forming alkyl–π FMGs. Chemical structure of the low-molecular-weight gelators, e) **GA1** and f) **GA2**, employed in this study.

To control G' of various alkyl–π FMLs such as alkylated naphthalene (**C₄C₈NL**,[29] **C₁₀C₁₄NL**, Figures 1a–i and 1a–ii), carbazole (**C₂C₆CZL**,[30] Figure 1a–iii), dicyanostyrylbenzene (**C₁₀C₁₄DCBL**,[20] Figure 1a–iv) and pyrene (**C₈C₁₂PL**, Figure 1a–v) were investigated in this study. **C₁₀C₁₄NL** (Supplementary Information, Scheme S1 and Figures S1–S5) and **C₈C₁₂PL** (Scheme S2, Figures S6–S13) were newly synthesized for this study. The above compounds are solvent-free neat liquids at room

temperature and are fluorescent, *e.g.*, blue, green, and light blue, derived from π-conjugated moieties under 365 nm ultraviolet (UV) light irradiation. The gels based on alkyl–π FMLs (FMGs) were prepared according to the scheme shown in Figure 1d. It is known that gelators having hydrogen-bonding units such as (*N*,*N*'-((1*S*,2*S*)-cyclohexane-1,2-diyl)didodecanamide) (**GA1**)[31] and (1-(2-benzylphenyl)-3-dodecyl urea) (**GA2**),[32] as shown in Figures 1e and 1f, cause gelation by forming fibrous self-assembled structures in solvents. **GA1**, which has two amide units and is known for effectively gelating low-polarity organic solvents[31,33] and liquid crystals,[34,35] was first employed to gelate five types of alkyl–π FMLs. In any combination, 1 wt% **GA1** was dissolved in the alkyl–π FMLs at 130 °C and formed transparent fluids. All combinations created physical gels confirmed by the vial inversion test[31–33] when cooling the mixture to room temperature. The gelation method successfully tuned *G*′ of alkyl–π FMLs by over five to seven orders of magnitude while maintaining the intrinsic fluorescence properties under UV light irradiation (Figure 1b, 1c, 2a, and S14). Since several types of FMLs with different π-moieties and substitution patterns can control different physical properties and functions [20,21,36,37], the gelation of these FMLs would benefit the future development of various applications of alkyl-π FMGs. Interestingly, the π-moiety content of the **C_2C_6CZL/GA1** gel reached 59 wt%.

Among these alkyl–π FMGs, we investigated the fundamental properties of gels based on **C_4C_8NL** and **$C_{10}C_{14}$NL**, the $|\eta^*|$ of which was 0.046 and 0.096 Pa s at 25 °C, respectively, and the effect of the alkyl chain length on the gels' physical properties was investigated. In addition to **GA1**, **GA2** was also tested for gelating **C_4C_8NL** and **$C_{10}C_{14}$NL**; thus, four alkyl–naphthalene FMGs were prepared. **GA2** has one urea unit, and it has been reported to gelate a wide range of liquids, from low-polarity organic solvents to ionic liquids.[32] The angular frequency (ω)-dependent rheological behavior of **C_4C_8NL** and its gel with 1 wt% **GA1** or **GA2** were evaluated (Figure 2a). **C_4C_8NL** exhibited a loss modulus (*G*″) over *G*′, and the slope of *G*″ was 1; it can be classified as a Newtonian liquid. When 1 wt% of **GA1** or **GA2** was added to **C_4C_8NL** and formed the gels, *G*′ increased by over seven orders of magnitude and became higher than *G*″ for both cases. In addition, *G*′ and *G*″ were almost independent of ω. Figures 2b and S15a show the strain (γ)-dependent rheology of the gels based on **C_4C_8NL** and **$C_{10}C_{14}$NL**, respectively, gelated by **GA1** or **GA2**. The rheological parameters of each gel are summarized in Table 1. Strains below about 0.2% exhibited a linear

viscoelastic region, and crossover points existed at strains between about 14% and 50%. The frequency-dependent and strain-dependent rheological properties are typical behavior of conventional gels formed by low-molecular-weight gelators.[32,38] **C_4C_8NL**-based gels have a higher *G′* and a lower tan *δ* than **$C_{10}C_{14}$NL**-based gels. Since the viscosity of **C_4C_8NL** is lower than that of **$C_{10}C_{14}$NL**, the gelator molecules in **C_4C_8NL** seemed to diffuse more easily in the sol–gel transition process during cooling, making it more suitable than **$C_{10}C_{14}$NL** for forming a well-structured fiber network.

Table 1. *G′*, *G″*, tan *δ*, and crossover point of the gels based on **C_4C_8NL** and **$C_{10}C_{14}$NL** with 1 wt% **GA1** or 1 wt% **GA2**

	C_4C_8NL /GA1	**$C_{10}C_{14}$NL /GA1**	**C_4C_8NL /GA2**	**$C_{10}C_{14}$NL /GA2**
G′ (kPa) [a]	28.7	13.5	20.8	19.3
G″ (kPa) [a]	3.82	2.36	5.22	5.18
tan *δ* [a][b]	0.133	0.176	0.251	0.268
Crossover point (%) [c]	39.1	41.9	48.9	14.0

[a] Strain = 0.1%, Angular frequency = 6.3 rad s^{-1}. [b] tan *δ* = *G″*/*G′*. [c] *γ* value when *G′* = *G″* in strain sweep measurement.

The fiber network structures of the gelators in **C_4C_8NL/GA1** and **C_4C_8NL/GA2** gels were confirmed by scanning electron microscopy (SEM, Figure 2c) for their xerogels prepared by extracting **C_4C_8NL** with *n*-hexane.[35] These fiber network structures contributed to the increase in *G′* of the alkyl–π FMLs. In the **C_4C_8NL/GA1** gel, as shown in Figure 2c–i, dense fibers were formed with an average thickness of 95 ± 28 nm (Figures 2c–i and S16), a similar thickness to that of the conventional organogels formed by **GA1**.[33] In contrast, in the xerogel prepared from the **C_4C_8NL/GA2** gel, the average thickness of the fibers was 363 ± 113 nm (Figures 2c–ii and S16). These differences in fiber thickness affect the transparency of the gels (Figures 2c and S15b).[33,39] The **C_4C_8NL/GA1** gel was transparent because of the fine and thinner fibers of **GA1**, whereas the **C_4C_8NL/GA2** gel was turbid due to the thicker fibers of **GA2** scattering the visible light. These results are also supported by powder X-ray diffraction (PXRD) and small- and wide-angle X-ray scattering (SWAXS) measurements (Figure S17).

The recovery behavior of a gel after it collapses due to an external force not only provides information about the molecular motion of the gelator but is also of practical importance. Hence, the thixotropy of the alkyl–naphthalene FMGs was investigated. After applying a 100% strain ($G'' > G'$), the recovery rate and recovery time of G' at 0.1% strain ($G' > G''$) were analyzed. The G' recovery rate of **C_4C_8NL/GA1**, **$C_{10}C_{14}$NL/GA1**, **C_4C_8NL/GA2**, and **$C_{10}C_{14}$NL/GA2** gels after 1 h from the 100% strain applied was confirmed to be 93%, 59%, 40%, and 24%, respectively (Figure S18). The G' of **C_4C_8NL** gels recovered more efficiently than that of **$C_{10}C_{14}$NL** gels. It is considered that the gels formed from the low-viscous **C_4C_8NL**, in which the gelator molecules can move/diffuse more easily to restore the self-assembled fiber network structures and recover G'. The G' recovery rates of the **GA2** gels were slower than those of **GA1**. Recovery of these gels from the collapsed state was much slower than that of conventional organogels, which completes the recovery in tens of seconds to several minutes.[40,41]

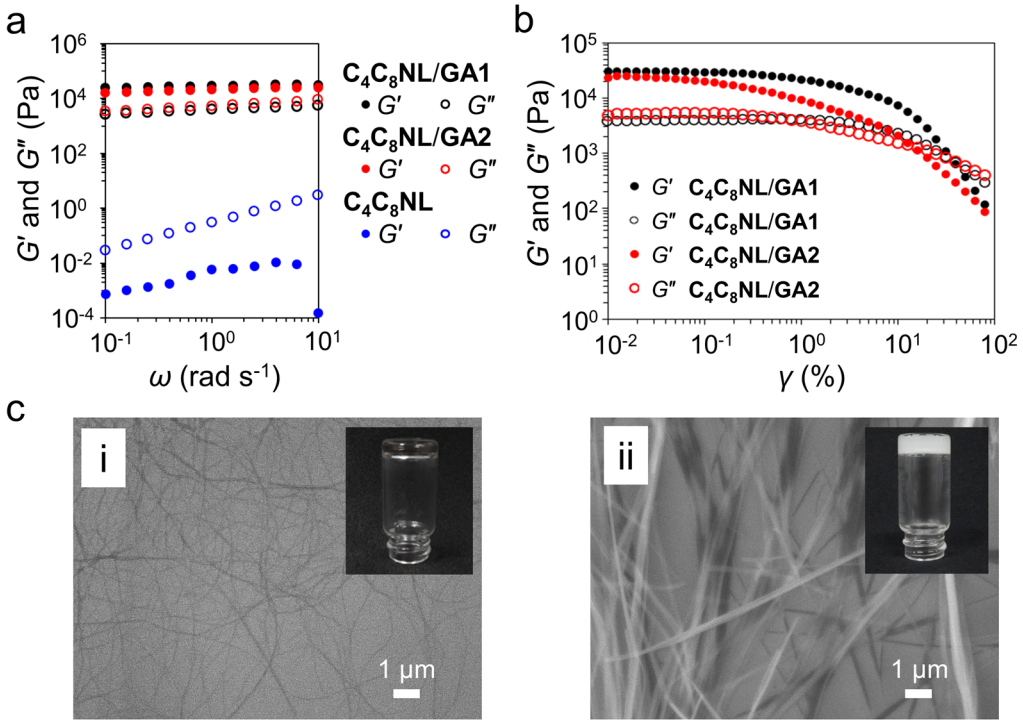

Figure 2. a) Angular frequency (ω)-dependent rheological behavior of **C_4C_8NL**, 1 wt% **C_4C_8NL/GA1** gel, and 1 wt% **C_4C_8NL/GA2** gel. b) Strain (γ)-dependent rheological behavior of 1 wt% **C_4C_8NL/GA1** gel and 1 wt% **C_4C_8NL/GA2** gel. c) Scanning electron microscopy (SEM) images of xerogels prepared from i) 1 wt% **C_4C_8NL/GA1** gel and ii) 1 wt% **C_4C_8NL/GA2** gel. Inset photo images are the corresponding gels under visible light.

The thermal stability of the obtained gels exhibited a similar trend to conventional organogels, such as concentration dependency (Figure S19) and weakening of the hydrogen bondings in the sol–gel transition (Figure S20).[42] The molecular dynamics of the gelated alkyl–naphthalene liquid molecules were evaluated by diffusion coefficient (*D*) measurement of the ^{1}H NMR stimulated echo method.[43–45] *D* is an index representing the degree of translational motion of a molecule. Figure 3a shows the *D* of **C_4C_8NL** molecules depending on the gelator concentration. **C_4C_8NL** exhibited a *D* of 1.67×10^{-11} m^2 s^{-1}. In the gel state, *D* decreased with an increase in the concentration of the gelator. Interfacial interactions near the gelator fibers could reduce the translational motion of **C_4C_8NL** molecules. In the case of **$C_{10}C_{14}$NL**, *D* did not decrease significantly after gelation, and little difference was observed between the gelator species types (Figure S21). This may be due to the higher viscosity, *i.e.*, slower translational motion of **$C_{10}C_{14}$NL** compared to **C_4C_8NL**, which makes it less susceptible to the gelator. In the **C_4C_8NL**/**GA2** gel, the *D* of **C_4C_8NL** is larger than that of the **C_4C_8NL**/**GA1** gel. This can be understood from the size of the gel fibers in their gels. The assembled thinner fibers of **GA1** have a more extensive interface area between the fibers and the **C_4C_8NL** molecules compared to that of the **C_4C_8NL**/**GA2** gel. Notably, the liquid molecules in the gels under any condition showed a *D* of about 80–90% compared to that of the neat liquid. Alkyl–π FMLs often exhibit functionalities unique to their fluidity, such as solvent functions and structural transitions.[37,46–52] Since fluidity is generally maintained even in the gel state, these alkyl–π FMGs are expected to exhibit functionalities based on the fluidity peculiar to alkyl–π FMLs.

Optical properties of neat alkyl–naphthalene liquids are also retained in the gel state. The absorption and fluorescence spectra of the gels exhibited almost identical features to those of the liquids (Figures 3b, S15c, and S22). The fluorescence quantum yield was also less affected by gelation (Table S1). In conventional π-gels consisting of organic solvent and gelator owning π-moieties, the content of the π-moieties is only a few wt% in the gels.[26,27] In contrast, alkyl–π FMGs are presumed to exhibit high functionality due to their high content of π-moieties. Regarding this point, we compared the fluorescence intensity between a conventional organogel and the **C_4C_8NL**/**GA1** gel. The content of the naphthyl moieties in organogels obtained by gelating *n*-hexane with 1 and 3 wt% of a gelator containing naphthyl groups (**GA3**,[53] Figure S23a) was only 0.2 and 0.6 wt%, respectively. In contrast, the **C_4C_8NL**/**GA1** gel

had a 40 wt% content of naphthyl moiety in the gel and emitted stronger fluorescence under UV light irradiation (Figures S23b and S23c). In addition, conventional organogels turn into xerogels in the air within a few hours because of the volatilization of organic solvents (Figure S23d). In contrast, alkyl–π FMLs have a low-volatility; thus, the FMGs can be stably handled in the air for a long period, *i.e.*, over a year in the dark at room temperature (23 ± 3 °C).

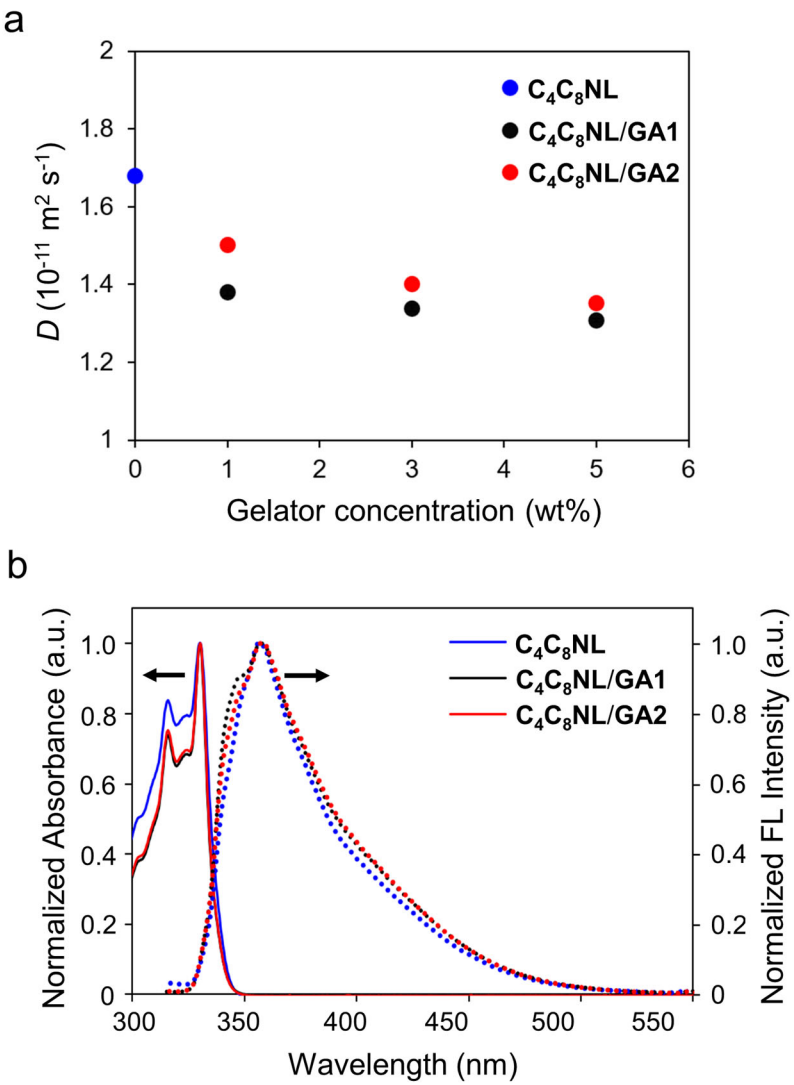

Figure 3. a) Diffusion coefficient of **C_4C_8NL** depending on the concentration of **GA1** and **GA2**. b) Normalized absorption (solid lines) and fluorescence (FL) spectra (dashed lines) of **C_4C_8NL**, 1 wt% **C_4C_8NL/GA1** gel, and 1 wt% **C_4C_8NL/GA2** gel.

Among the alkyl–π FMLs, **C_8C_{12}PL** is suitable for an electret application because a relatively wide π-conjugated unit is entirely covered with insulating alkyl chains (Figure S24a and Table S2), as reported in the electretization of alkyl–porphyrin[18]

and alkyl–fullerene liquids.[16] Since bleeding causes a problem when forming MEGs with alkyl–π FMLs,[18] fabrication with the gel state is advantageous for constructing highly durable MEGs. First, we evaluated the charge retention capacity. The polyurethane (PU) nonwoven fabric impregnated with **C_8C_{12}PL** (Figure S25) and **C_8C_{12}PL/GA1** (1 wt%) gel (Figure S26) was electrified by positive corona discharging at 100 °C for 30 min, and then charging was continued for over 30 min until cooling to room temperature (Figure S24b). **C_8C_{12}PL/GA1** gel exhibited an electrical charge of 0.12 C m^{-3}, approximately 24% larger than **C_8C_{12}PL** (0.097 C m^{-3}), and had a longer charge retention (Figure 4a). Since **GA1** alone shows only a little charge retention, enhancement of electret performance by gelation is considered to result from the increase in G'. In this positive corona discharging process, electrification occurs during the process from sol to gel transition; therefore, charged species, *e.g.*, $N_2^{+\bullet}$, $O_2^{+\bullet}$, $H_3O^{+\bullet}$, could be efficiently captured in the **C_8C_{12}PL/GA1** gel, resulting in higher electret performance. The charge density of the **C_8C_{12}PL/GA1** gel was three times higher than that of a typical stretchable polymer electret (0.04 C m^{-3}).[54]

MEGs were fabricated using PU nonwoven fabric impregnated with **C_8C_{12}PL** and **C_8C_{12}PL/GA1** gel (Figure 4b). The PU nonwoven fabric was sandwiched between deformable silver electrodes and a PU masking layer. The device was approximately 130 mg in weight and 200 μm in thickness. Figure 4c explains the mechanism of mechanoelectric generation. When a force is applied to push the device, the distance between the electrodes is reduced, resulting in an electric current. The device formed with the **C_8C_{12}PL/GA1** gel exhibited an open-circuit voltage (V_{OC}) about 83 ± 4% higher than the **C_8C_{12}PL**-based MEG under a continuously applied 16.7 Hz vibration (Figures 4d, 4e, and S27a, Table S3). Regarding the change in V_{OC} over the course of days, the gel device maintained a higher V_{OC} than the liquid one (Figure S28). When we utilize liquid materials for electrets,[16,18] we must impregnate them into the nonwoven supporting fabric to prevent short circuits due to contact between the electrodes (Figure S27b). In contrast, there is no contact between electrodes even without the supporting fabric in the case of gels with improved elasticity compared to liquids, and it showed a vibration power generation function of 64 ± 5% V_{OC} compared to the device with supporting fabric (Figure 4f and Table S3). When a vibration of 16.7 Hz was applied to the **C_8C_{12}PL/GA1** gel in a vial, the gel shape was maintained (Supplementary movies S1 and S2). In addition, the V_{OC} of the gel device was almost

constant even when the continuous vibration was applied for 10 min (Figure S27c). Therefore, during the MEG operation, gel collapse may not occur. Importantly, no liquid leakage from the gel MEG devices was observed. Furthermore, since the gel MEG device is deformable, it worked even when folded or bent (Figures S27d–h).

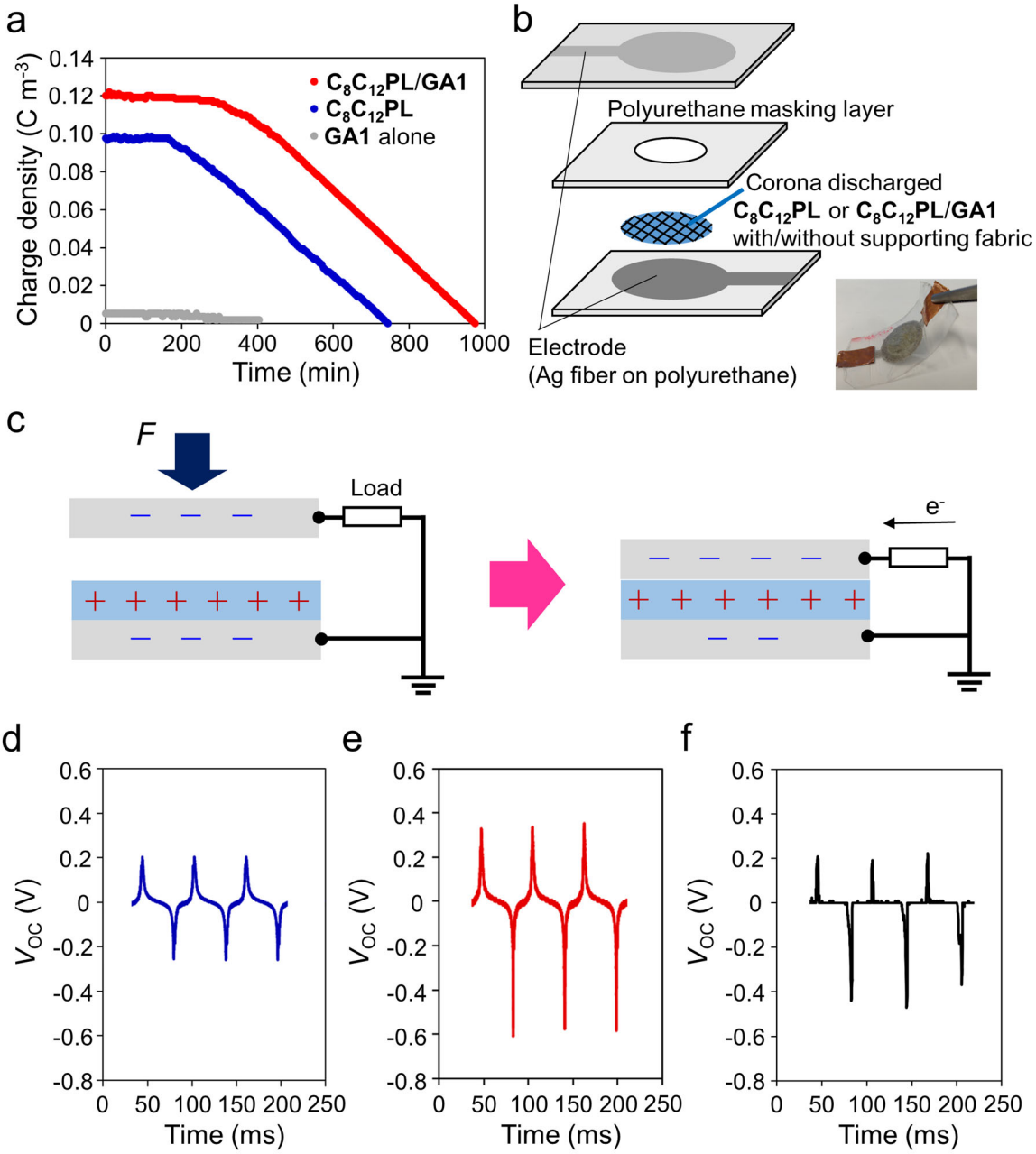

Figure 4. a) Changes over time in the charge amount of nonwoven fabric containing **C_8C_{12}PL** liquid and **C_8C_{12}PL/GA1** gel after corona discharge measured by a Coulomb meter. b) Device structure and photo image of MEG. c) Mechanism of mechanoelectric generation. Waveform of open-circuit voltage of MEGs fabricated with d) **C_8C_{12}PL**, 1 wt% **C_8C_{12}PL/GA1** gel e) with and f) without supporting fabric, when continuous vibration (frequency = 16.7 Hz) was applied.

In conclusion, we developed a method for controlling *G′* of alkyl–π FMLs by gelation, *i.e.*, the formation of alkyl–π FMGs. Blue, green, and light blue fluorescent alkyl–π FMLs were gelated by low-molecular-weight gelators having hydrogen-bonding units. The *G′* of these liquids was increased by five to seven orders of magnitude while retaining their optical properties. The sol–gel transition temperature and rheological properties can be modulated by the alkyl chain length of the alkyl–π FMLs and the species of the gelators; however, *D* of more than 80% compared to the liquids was preserved in the gels. This suggests that the fluidity of the liquid molecules is well maintained in the gel state, although *G′* of the materials changes significantly. The alkyl–pyrene FMG worked for mechanoelectric generation without liquid leakage and even without supporting fabric, and its performance was remarkably improved compared with the device with the liquid. Using gelation, *G′* of the alkyl–π FMLs could be adjusted to a region close to the range of *G′* of human body organs (10^1 to 10^5 Pa).[55] Therefore, this technique will expand the potential of alkyl–π FMLs/FMGs for biological applications. To further expand the types of alkyl–π FMGs and realize more advanced functions, it is necessary to introduce stimuli-responsive units into gelator molecules.[56–64] These attempts will enable the development of novel alkyl–π FMGs that can be applied to various fields such as healthcare, sensing, and soft-robotics.

Acknowledgments

This work was supported by the World Premier International Research Center Initiative (WPI), MEXT, Japan. We thank Ms. Keiko Sano and Dr. Xiao Zheng (NIMS) for their cooperation in the synthesis of **C_8C_{12}PL** and **$C_{10}C_{14}$DCBL**, respectively, Dr. Naoaki Kuwata (NIMS) for assistance with the diffusion coefficient measurement, and Dr. Akira Shinohara (NIMS) for insightful discussions.

Conflicts of interest

There are no conflicts to declare.

Data Availability Statement

The data that support this study are available in the supplementary material of this article.

Keywords: π-gel • functional molecular liquid • low-molecular-weight gelator • luminescence • electret

References

[1] C. Majidi, *Adv. Mater. Technol.* **2018**, 1800477.

[2] T. Someya, Z. Bao, G. G. Malliaras, *Nature* **2016**, *540*, 379–385.

[3] C. Wang, C. Wang, Z. Huang, S. Xu, *Adv. Mater.* **2018**, *30*, 1801368.

[4] Y. Jiang, Z. Zhang, Y.-X. Wang, D. Li, C.-T. Coen, E. Hwaun, G. Chen, H.-C. Wu, D. Zhong, S. Niu, W. Wang, A. Saberi, J.-C. Lai, Y. Wu, Y. Wang, A. A. Trotsyuk, K. Y. Loh, C.-C. Shih, W. Xu, K. Liang, K. Zhang, Y. Bai, G. Gurusankar, W. Hu, W. Jia, Z. Cheng, R. H. Dauskardt, G. C. Gurtner, J. B.-H. Tok, K. Deisseroth, I. Soltesz, Z. Bao, *Science* **2022**, *375*, 1411–1417.

[5] J. Xu, S. Wang, G.-J. N. Wang, C. Zhu, S. Luo, L. Jin, X. Gu, S. Chen, V. R. Feig, J. W. F. To, S. Rondeau-Gagné, J. Park, B. C. Schroeder, C. Lu, J. Y. Oh, Y. Wang, Y.-H. Kim, H. Yan, R. Sinclair, D. Zhou, G. Xue, B. Murmann, C. Linder, W. Cai, J. B.-H. Tok, J. W. Chung, Z. Bao, *Science* **2017**, *355*, 59–64.

[6] C. Larson, B. Peele, S. Li, S. Robinson, M. Totaro, L. Beccai, B. Mazzolai, R. Shepherd, *Science* **2016**, *351*, 1071–1074.

[7] M. Ha, S. Lim, H. Ko, *J. Mater. Chem. B* **2018**, *6*, 4043–4064.

[8] A. Shinohara, Z. Guo, C. Pan, T. Nakanishi, *Org. Mater.* **2021**, *3*, 309–320.

[9] S. E. Root, S. Savagatrup, A. D. Printz, D. Rodriquez, D. J. Lipomi, *Chem. Rev.* **2017**, *117*, 6467–6499.

[10] A. Ghosh, T. Nakanishi, *Chem. Commun.* **2017**, *53*, 10344–10357.

[11] F. Lu, T. Nakanishi, *Adv. Opt. Mater.* **2019**, *7*, 1900176.

[12] F. Lu, T. Nakanishi, *Sci. Technol. Adv. Mater.* **2015**, *16*, 014805.

[13] *Functional Organic Liquids* (Ed.: T. Nakanishi), Wiley-VCH, Weinheim, **2019**.

[14] T. Kasahara, S. Matsunami, T. Edura, J. Oshima, C. Adachi, S. Shoji, J. Mizuno, *Sens. Actuators A Phys.* **2013**, *195*, 219–223.

[15] N. Kobayashi, T. Kasahara, T. Edura, J. Oshima, R. Ishimatsu, M. Tsuwaki, T. Imato, S. Shoji, J. Mizuno, *Sci. Rep.* **2015**, *5*, 14822.

[16] R. K. Gupta, M. Yoshida, A. Saeki, Z. Guo, T. Nakanishi, *Mater. Horiz.* **2023**, *10*, 3458–3466.

[17] A. Shinohara, M. Yoshida, C. Pan, T. Nakanishi, *Polym. J.* **2023**, *55*, 529–535.

[18] A. Ghosh, M. Yoshida, K. Suemori, H. Isago, N. Kobayashi, Y. Mizutani, Y. Kurashige, I. Kawamura, M. Nirei, O. Yamamuro, T. Takaya, K. Iwata, A. Saeki, K. Nagura, S. Ishihara, T. Nakanishi, *Nat. Commun.* **2019**, *10*, 4210.

[19] Z. Guo, Y. Patil, A. Shinohara, K. Nagura, M. Yoshida, T. Nakanishi, *Mol. Syst. Des. Eng.* **2022**, *7*, 537–552.

[20] X. Zheng, K. Nagura, T. Takaya, K. Hashi, T. Nakanishi, *Chem. Eur. J.* **2023**, *29*, e202203775.

[21] F. Lu, T. Takaya, K. Iwata, I. Kawamura, A. Saeki, M. Ishii, K. Nagura, T. Nakanishi, *Sci. Rep.* **2017**, *7*, 3416.

[22] V. C. Wakchaure, S. D. Veer, A. D. Nidhankar, V. Kumar, A. Narayanan, S. S. Babu, *Angew. Chem. Int. Ed.* **2023**, *62*, e202307381; *Angew. Chem.* **2023**,*135*, e202307381.

[23] Z. Guo, A. Shinohara, C. Pan, F. J. Stadler, Z. Liu, Z.-C. Yan, J. Zhao, L. Wang, T. Nakanishi, *Mater. Horiz.* **2020**, *7*, 1421–1426.

[24] A. Shinohara, C. Pan, Z. Guo, L. Zhou, Z. Liu, L. Du, Z. Yan, F. J. Stadler, L. Wang, T. Nakanishi, *Angew. Chem. Int. Ed.* **2019**, *58*, 9581–9585; *Angew. Chem.* **2019**, *131*, 9682–9686.

[25] R. Laishram, S. Sarkar, I. Seth, N. Khatun, V. K. Aswal, U. Maitra, S. J. George, *J. Am. Chem. Soc.* **2022**, *144*, 11306–11315.

[26] S. Panja, D. J. Adams, *Chem. Soc. Rev.* **2021**, *50*, 5165–5200.

[27] S. S. Babu, V. K. Praveen, A. Ajayaghosh, *Chem. Rev.* **2014**, *114*, 1973–2129.

[28] R. G. Weiss, *J. Am. Chem. Soc.* **2014**, *136*, 7519–7530.

[29] B. Narayan, K. Nagura, T. Takaya, K. Iwata, A. Shinohara, H. Shinmori, H. Wang, Q. Li, X. Sun, H. Li, S. Ishihara, T. Nakanishi, *Phys. Chem. Chem. Phys.* **2018**, *20*, 2970–2975.

[30] E. Hendrickx, B. D. Guenther, Y. Zhang, J. F. Wang, K. Staub, Q. Zhang, S. R. Marder, B. Kippelen, N. Peyghambarian, *Chem. Phys.* **1999**, *245*, 407–415.

[31] K. Hanabusa, M. Yamada, M. Kimura, H. Shirai, *Angew. Chem. Int. Ed.* **1996**, *35*, 1949–1951; *Angew. Chem.* **1996**, *108*, 2086–2088.

[32] T. Komiyama, Y. Harada, T. Hase, S. Mori, S. Kimura, M. Yokoya, M. Yamanaka, *Chem. Asian. J.* **2021**, *16*, 1750–1755.

[33] H. Nakagawa, M. Fujiki, T. Sato, M. Suzuki, K. Hanabusa, *Bull. Chem. Soc. Jpn.* **2017**, *90*, 312–321.

[34] T. Kato, T. Kutsuna, K. Hanabusa, M. Ukon, *Adv. Mater.* **1998**, *10*, 606–608.

[35] K. Yabuuchi, A. E. Rowan, R. J. M. Nolte, T. Kato, *Chem. Mater.* **2000**, *12*, 440–443.

[36] Y. Yamamoto, F. Lu, T. Nakanishi, S. Hayashi, *J. Phys. Chem. B* **2023**, *127*, 4870–4885.

[37] A. Tateyama, T. Nakanishi, *Responsive Mater.* **2023**, *1*, e20230001.

[38] H. Sawada, M. Yamanaka, *Chem. Asian. J.* **2018**, *13*, 929–933.

[39] J. N. Loos, C. E. Boott, D. W. Hayward, G. Hum, M. J. Maclachlan, *Langmuir* **2021**, *37*, 105–114.

[40] A. Dawn, H. Kumari, *Chem. Eur. J.* **2018**, *24*, 762–776.

[41] Y. Ohsedo, M. Oono, A. Tanaka, H. Watanabe, *New J. Chem.* **2013**, *37*, 2250.

[42] N. Mohmeyer, H.-W. Schmidt, *Chem. Eur. J.* **2007**, *13*, 4499–4509.

[43] J. Kowalczuk, A. Rachocki, M. Bielejewski, J. Tritt-Goc, *J. Colloid Interface Sci.* **2016**, *472*, 60–68.

[44] M. Yemloul, E. Steiner, A. Robert, S. Bouguet-Bonnet, F. Allix, B. Jamart-Grégoire, D. Canet, *J. Phys. Chem. B* **2011**, *115*, 2511–2517.

[45] J. Kowalczuk, S. Jarosz, J. Tritt-Goc, *Tetrahedron* **2009**, *65*, 9801–9806.

[46] M. J. Hollamby, M. Karny, P. H. H. Bomans, N. A. J. M. Sommerdjik, A. Saeki, S. Seki, H. Minamikawa, I. Grillo, B. R. Pauw, P. Brown, J. Eastoe, H. Möhwald, T. Nakanishi, *Nat. Chem.* **2014**, *6*, 690–696.

[47] S. S. Babu, M. J. Hollamby, J. Aimi, H. Ozawa, A. Saeki, S. Seki, K. Kobayashi, K. Hagiwara, M. Yoshizawa, H. Möhwald, T. Nakanishi, *Nat. Commun.* **2013**, *4*, 1969.

[48] S. S. Babu, J. Aimi, H. Ozawa, N. Shirahata, A. Saeki, S. Seki, A. Ajayaghosh, H. Möhwald, T. Nakanishi, *Angew. Chem. Int. Ed.* **2012**, *51*, 3391–3395; *Angew. Chem.* **2012**, *124*, 3447–3451.

[49] A. Ikenaga, Y. Akiyama, T. Ishiyama, M. Gon, K. Tanaka, Y. Chujo, K. Isoda, *ACS Appl. Mater. Interfaces* **2021**, *13*, 47127–47133.

[50] K. Isoda, Y. Sato, D. Matsukuma, *ChemistrySelect* **2017**, *2*, 7222–7226.

[51] T. Ogoshi, K. Maruyama, Y. Sakatsume, T. Kakuta, T. Yamagishi, T. Ichikawa, M. Mizuno, *J. Am. Chem. Soc.* **2019**, *141*, 785–789.

[52] X. Zheng, R. K. Gupta, T. Nakanishi, *Curr. Opin. Colloid Interface Sci.* **2022**, *62*, 101641.

[53] X. Wang, P. Duan, M. Liu, *Chem. Asian. J.* **2014**, *9*, 770–778.

[54] S. Zhang, Y. Wang, X. Yao, P. L. Floch, X. Yang, J. Liu, Z. Suo, *Nano Lett.* **2020**, *20*, 4580–4587.

[55] T. R. Cox, J. T. Erler, *Dis. Models Mech.* **2011**, *4*, 165–178.

[56] M. Martínez-Abadía, R. K. Dubey, M. Fernández, M. Martín-Arroyo, R. Aguirresarobe, A. Saeki, A. Mateo-Alonso, *Chem. Sci.* **2022**, *13*, 10773–10778.

[57] M. Kawaura, T. Aizawa, S. Takahashi, H. Miyasaka, H. Sotome, S. Yagai, *Chem. Sci.* **2022**, *13*, 1281–1287.

[58] S. M. M. Reddy, P. Dorishetty, G. Augustine, A. P. Deshpande, N. Ayyadurai, G. Shanmugam, *Langmuir* **2017**, *33*, 13504–13514.

[59] S. Mukherjee, T. Kar, P. K. Das, *Chem. Asian. J.* **2014**, *9*, 2798–2805.

[60] M. K. Nayak, *J. Photochem. Photobiol. A* **2011**, *217*, 40–48.

[61] C. Vijayakumar, V. K. Praveen, A. Ajayaghosh, *Adv. Mater.* **2009**, *21*, 2059–2063.

[62] T. Kitahara, N. Fujita, S. Shinkai, *Chem. Lett.* **2008**, *37*, 912–913.

[63] K. Yabuuchi, Y. Tochigi, N. Mizoshita, K. Hanabusa, T. Kato, *Tetrahedron* **2007**, *63*, 7358–7365.

[64] S. J. George, A. Ajayaghosh, *Chem. Eur. J.* **2005**, *11*, 3217–3227.